



Discover Generics

Cost-Effective CT & MRI Contrast Agents



WATCH VIDEO

AJNR







This information is current as of June 2, 2025.

Modeling Robotic-Assisted Mechanical Thrombectomy Procedures with the CorPath GRX Robot: The Core-Flow Study

Alejandro Tomasello, David Hernández, Jiahui Li, Riccardo Tiberi, Eila Rivera, Joan Daniel Vargas, Cristina Losada, Magda Jablonska, Marielle Esteves, Maria Lourdes Diaz, Judith Cendrero, Manuel Requena, Francesco Diana, Marta De Dios, Trisha Singh, Laura Ludovica Gramegna and Marc Ribo

AJNR Am J Neuroradiol published online 25 April 2024
<http://www.ajnr.org/content/early/2024/04/25/ajnr.A8205>

Modeling Robotic-Assisted Mechanical Thrombectomy Procedures with the CorPath GRX Robot: The Core-Flow Study

Alejandro Tomasello,  David Hernández, Jiahui Li,  Riccardo Tiberi, Eila Rivera, Joan Daniel Vargas, Cristina Losada,  Magda Jablonska, Marielle Esteves, Maria Lourdes Diaz, Judith Cendrero,  Manuel Requena,  Francesco Diana, Marta De Dios, Trisha Singh, Laura Ludovica Gramegna, and  Marc Ribo



ABSTRACT

BACKGROUND AND PURPOSE: Endovascular robotic devices may enable experienced neurointerventionalists to remotely perform endovascular thrombectomy. This study aimed to assess the feasibility, safety, and efficacy of robot-assisted endovascular thrombectomy compared with manual procedures by operators with varying levels of experience, using a 3D printed neurovascular model.

MATERIALS AND METHODS: M1 MCA occlusions were simulated in a 3D printed neurovascular model, linked to a CorPath GRX robot in a biplane angiography suite. Four interventionalists performed manual endovascular thrombectomy ($n = 45$) and robot-assisted endovascular thrombectomy ($n = 37$) procedures. The outcomes included first-pass recanalization (TICI 2c–3), the number and size of generated distal emboli, and procedural length.

RESULTS: A total of 82 experimental endovascular thrombectomies were conducted. A nonsignificant trend favoring the robot-assisted endovascular thrombectomy was observed in terms of final recanalization (89.2% versus manual endovascular thrombectomy, 71.1%; $P = .083$). There were no differences in total mean emboli count (16.54 [SD, 15.15] versus 15.16 [SD, 16.43]; $P = .303$). However, a higher mean count of emboli of > 1 mm was observed in the robot-assisted endovascular thrombectomy group (1.08 [SD, 1.00] versus 0.49 [SD, 0.84]; $P = .001$) compared with manual endovascular thrombectomy. The mean procedural length was longer in robot-assisted endovascular thrombectomy (6.43 [SD, 1.71] minutes versus 3.98 [SD, 1.84] minutes; $P < .001$). Among established neurointerventionalists, previous experience with robotic procedures did not influence recanalization (95.8% were considered experienced; 76.9% were considered novices; $P = .225$).

CONCLUSIONS: In a 3D printed neurovascular model, robot-assisted endovascular thrombectomy has the potential to achieve recanalization rates comparable with those of manual endovascular thrombectomy within competitive procedural times. Optimization of the procedural setup is still required before implementation in clinical practice.


ABBREVIATIONS: BGC = balloon guide catheter; EVT = endovascular thrombectomy; MA = manual; MT = mechanical thrombectomy; RA = robot-assisted; SR = stent retriever

Mechanical thrombectomy (MT) is the most effective treatment for acute ischemic stroke due to large-vessel occlusion when combined with IV-tPA, unless contraindicated, and is currently strongly recommended by all therapeutic guidelines.^{1,2}

Received August 29, 2023; accepted after revision January 12, 2024.

From the Interventional Neuroradiology Section (A.T., D.H., J.D.V., C.L., M. Requena, F.D., M.D.D., T.S.), Stroke Research (J.L., R.T., M.J., J.C., M. Requena, M. Ribo) Vall d'Hebron Institut de Recerca (E.R., F.D., L.L.G.), Stroke Unit (M. Requena, M. Ribo), Neurology Department Experimental Surgery Unit (M.E.), Vall d'Hebron Barcelona Hospital Campus, Barcelona, Spain; Departamento de Medicina (A.T.), Universitat Autònoma de Barcelona, Barcelona, Spain; 2nd Department of Radiology (M.J.), Medical University of Gdańsk, Gdańsk, Poland; and Departament De Radiologia Vascular Interventista (M.L.D.), Hospital General Universitario Arnau de Villanova, Lleida, Spain.

Please address correspondence to Alejandro Tomasello, MD, Interventional Neuroradiology Section, Vall d'Hebron University Campus Hospital, Pg. Vall d'Hebron, 119-129 08035 Barcelona, Spain; e-mail: alejandrotomasello@gmail.com

 Indicates article with online supplemental data.

<http://dx.doi.org/10.3174/ajnr.A8205>

However, logistic and geographic limitations in the availability of rapid performance of the thrombectomy procedure create geographic inequities among territories due to the procedure being more accessible in urban areas than in remote rural locations distant from major cities.²⁻⁴ Appropriate MT programs require not only modern angiography suites but also certified physicians who are well-trained in neurointerventional procedures and remain in continual contact with the neuroscientific society; this scenario ensures the highest-quality standards. In recent years, endovascular robotic devices have emerged as a revolutionary technology that may transform the field of neurointerventional treatment.

The CorPath GRX System (Corindus) is the first FDA-cleared and CE Marked medical device for percutaneous coronary and vascular procedures. It uses articulated robotic arms with multiple degrees of freedom to handle microguidewires and microcatheters, enabling submillimeter movements of both devices to

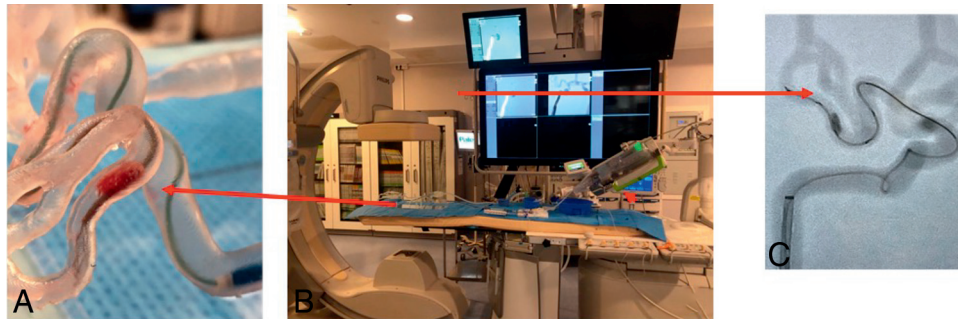


FIG 1. A benchtop 3D printed vascular model with a thrombus inside (A) was connected to a Corindus CorPath GRX robot (B, arrowhead), and MT was performed using SRs (C).

perform precise neurovascular interventions. Physicians can control it remotely, reducing radiation exposure and providing a comfortable and more precise working distance.⁵⁻⁷

Studies focusing on the embolization of intracranial aneurysms have been published dating back to the first-in-human experience reported in 2018, in which a transradial diagnostic coronary angiography was performed.^{6,7}

The potential use of robotic treatment in stroke thrombectomy procedures could represent a substantial advancement in stroke treatment, providing an alternative solution for patients in nonurban areas. Robot-assisted endovascular thrombectomy (RA-EVT) could save time by avoiding long transfers; it also offers patients the possibility of being treated remotely by highly-skilled neurointerventionalists, ultimately improving patient outcomes and quality of life. Although the CorPath GRX, which is capable of performing biaxial procedures, is not fully optimized for thrombectomy procedures, it allows multiple catheter maneuvers and yields an accuracy comparable—or superior—to manual procedures.

The present study aims to describe a potential setup and explore the feasibility (reaching the occlusion), safety (distal embolization), and efficacy (recanalization) of RA-EVT compared with manual procedures performed by operators with varying levels of experience in robotics, using a 3D printed neurovascular model.

MATERIALS AND METHODS

Study Design

Two neurointerventionalists with >3 years of clinical experience in robotic-assisted neuroendovascular embolizations (ie, robot-experienced) performed both manual EVT (MA-EVT, $n = 18$) and RA-EVT ($n = 24$). One experienced neurointerventionalist in training for the robotic procedure (ie, robot-novice) performed both MA-EVT ($n = 6$) and RA-EVT ($n = 13$) procedures. Due to the exploratory nature of this pilot feasibility study, the total number of experiments performed by each interventionalist was not predefined on the basis of efficacy assumption; a total number between 19 and 21 experiments per operator was decided.

Neurovascular Flow Loop Model

The neurovascular model was based on the vascular anatomies extracted from anonymized CTA images. The manufacturing procedure comprises the following steps: medical image segmentation to generate the preliminary 3D geometry of the vascular anatomy; mesh modeling to simplify the anatomy and prepare a

printable model; 3D printing setting; postprinting processing; and assembly.

Data in the DICOM format was imported and loaded in 3D Slicer (<http://www.slicer.org>),^{8,9} where opacity threshold segmentation was performed to obtain the preliminary 3D geometry of the model. The preliminary 3D geometry was exported to Autodesk Meshmixer (<https://meshmixer.com/>)¹⁰ for the modeling stage and exported to PreForm (Formlabs) to configure the printing material, resolution, optimal geometry orientation, and support structure for 3D printing. The model was printed with commercially available photopolymer resin Elastic 50A at a resolution of 100 μm with a Form 3 SLA printer (Formlabs). The postprinting process consisted of removing support structures from the model, a 10-minute dip in isopropyl alcohol, and exposure to 305-nm ultraviolet light at a temperature of 60°C for 10 minutes. After the postprocessing, the model parts were assembled to constitute the final version of the neurovascular model, which includes the aortic arch, bilateral carotid arteries, MCAs (up to 2 distal M2 MCA branches), anterior cerebral arteries (up to the proximal A2), anterior communicating artery, posterior communicating arteries, and posterior cerebral arteries (up to the proximal P2 posterior cerebral artery segments).

The neurovascular model was connected in a flow-loop setup to mimic blood circulation. The experimental setup comprised a hydraulic pump recirculating saline solution at 800 mL/min, a 3D printed model, and a 100- μm filter at the outflow of the model to collect the periprocedural emboli. All elements were connected through a silicone tubing system. To simulate the transfemoral access, we connected an 8F sheath attached to a silicone tube to the descending aorta. An inflow filter was added between the hydraulic pump and the neurovascular model to filter out the undesired particles introduced into the system by reused devices.

Experimental Thrombectomy Setup

The study was performed using biplane angiography (Clarity, Philips Healthcare): As previously described,¹¹ 2 \times 4 mm (radioopaque) clot analogs were made from porcine blood and used to create arterial occlusions in a benchtop 3D printed model (Fig 1A).¹²

The CorPath CRX robot, consisting of a control console and a robotic unit equipped with an extension arm that can hold a single-use cassette, was installed in the interventional neuroradiology section. The control console, enabling the operator to perform procedures comfortably while seated, was placed in the RX control

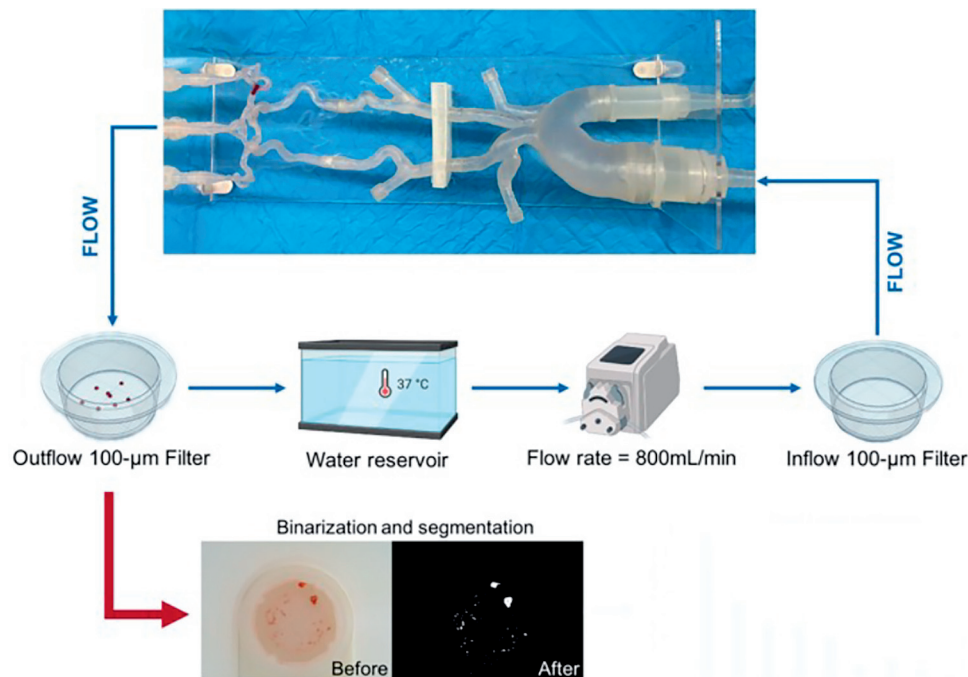


FIG 2. Experimental setup for robot-assisted and manual EVTs.

room. The extension arm and robotic unit were positioned on the lateral side of the table in the angiosuite. A single-use cassette was loaded with a microcatheter and a balloon guide catheter (BGC) (Gateway; Stryker), both of which were connected to the neurovascular model.

The robotic system is currently unable to perform catheterization of the aortic arch because it is limited to an advancement movement of 20 cm. An initial assessment of the optimal positioning of the different devices was performed. Due to the above-mentioned limited range of movement of the microcatheter when using the robot, the limiting factor to reach and cross the clot with the microcatheter is the initial position of the BGC in the ICA. We identified the lowest point in the ICA in which the tip of the BGC should be manually positioned before initiating the RA-EVT for different occlusion locations (Fig 2) and decided to place it in the vertical part of the petrous segment of the ICA. Given this limitation, RA-EVT was considered optimal for occlusions located in the ICA and in the M1 segment of the MCA and in any case beyond the proximal M2 branches.

After clot embolization, experiments were allocated into one of the following treatment arms: 1) robot-experienced/MA-EVT; 2) robot-experienced/RA-EVT; 3) robot-novice/MA-EVT; 4) robot-novice/RA-EVT. A 6F BGC was manually advanced by an experienced specialist nurse to the level of the distal ICA, then a 0.021-inch microcatheter (Phenom 21; Medtronic) was manually advanced to the level of the tip of the BGC. For RA-EVT procedures, the microcatheter and a 0.014-inch microguidewire (Synchro 2; Stryker) were then connected to the CorPath GRX robot by a trained assistant nurse; the neurointerventionalist could take control of the system from the console located in the control room outside the angiosuite (Fig 1).

The thrombectomy technique, manual and robot-assisted, consisted of navigating the microcatheter under fluoroscopy to the

MCA to cross the clot and then deploy a 4×40 mm stent retriever (SR; Solitaire X; Medtronic) from the M2 to the M1 segment of the MCA. After an embedding time of 1–2 minutes, the BGC was inflated and the SR was retrieved into the BGC under proximal flow arrest and continuous pump aspiration (Penumbra) (Fig 1C). For RA-EVT device exchanges in the robotic system, balloon inflation/deflation and aspiration were performed at the neurointerventionalist's indication, executed by an assistant nurse.

Each experiment consisted of a single pass per embolized clot. The primary outcome was first-pass recanalization (TICI 2c–3); the secondary outcome was the characterization of the collected distal emboli after each experiment.¹³ The duration of the MT procedure was defined as the moment when the neurointerventionalist first initiated control of the console and began maneuvering the microcatheter, until completion of the first pass.

Characterization of Distal Emboli

Characterization of generated distal emboli has been performed as previously described.¹² The distal segments of the neurovascular model have vessels as narrow as 1 mm. Thus, most embolized particles would end up in the filter located at the outflow of the model. An RGB image of the particles in the filter was captured with a high-resolution digital camera (IPEVO, Inc., Sunnyvale, California) to analyze the emboli generated after each pass. Then, the RGB images were processed by an image-processing algorithm developed on Matlab R2020a (MathWorks). The algorithm comprises 2 primary stages: 1) RGB image binarization, which involves highlighting the emboli (“1”) and removing the background (“0”) (Fig 2); and 2) quantification of the major-axis length of each particle, using a circle of known dimensions as a reference. Additionally, the algorithm provides output such as the overall particle count as well as the number of emboli of >1 mm.

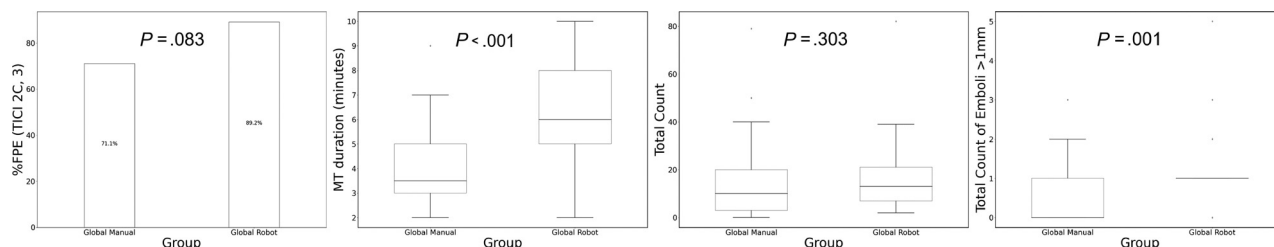


FIG 3. Boxplot analysis shows the difference in median values of various outcomes of thrombectomy (such as recanalization rate, procedural length, and distal emboli generation) when comparing all RA-EVTs and all MA-EVTs. FPE indicates first-pass effect.

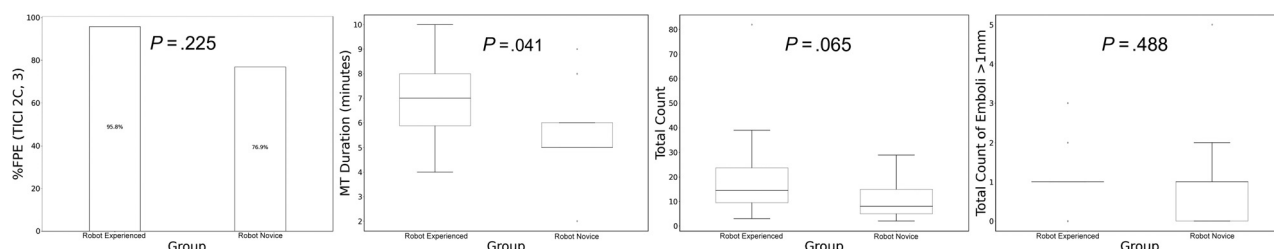


FIG 4. Boxplot analysis shows the difference in median values of various outcomes of thrombectomy (such as recanalization rate, procedural length, and distal emboli generation) when comparing robotic-EVT performed by a robotic-experienced interventional neuroradiologist and robotic-EVT performed by a robot-novice interventional neuroradiologist. FPE indicates first-pass effect.

Statistical Analysis

Results were expressed as mean (SD). Data were analyzed using the SciPy library from Python (<https://scipy.org/>). Normality was tested with Shapiro-Wilk test, and the Mann-Whitney *U* test was used to evaluate differences between RA-EVTs and MA-EVTs. Multiple subgroup analyses were performed to assess the safety and efficacy of the procedure among the 4 treatment arms using a χ^2 test.

As a subgroup analysis, differences in different outcomes (ie, final recanalization rate, number and dimension of emboli, and duration of the MT procedure) were compared between RA-EVT performed by a robot-experienced interventionalist and RA-EVT performed by a robot-novice neurointerventionalist who all had the same levels of experience in MT procedures (>10 years).

Statistical significance was $P < .05$.

RESULTS

We conducted a total of 82 experimental EVT: 37 RA-EVTs and 45 MA-EVTs. Each interventionalist performed between 19 and 21 experiments. There were no robotic system failures or incidents that required the technician to step in during the thrombectomy attempts.

Robot-Assisted EVT versus Manual EVT

Overall, when comparing all RA-EVTs ($n = 37$) versus all MA-EVTs ($n = 45$), nonsignificant trends were observed in terms of the final recanalization rate in favor of RA-EVT: 89.2% versus MA-EVT: 71.1%; $P = .083$. The distal emboli analysis revealed a similar mean total count of particles (RA-EVT: 16.54 [SD, 15.15] versus MA-EVT: 15.16 [SD, 16.43]; $P = .303$); however, a significantly mean higher number of emboli of >1 mm in diameter were observed in the RA-EVT (1.08 [SD, 1] versus 0.49 [SD, 0.84]; $P = .001$). In addition, the mean RA-EVT procedural length was

significantly longer (RA-EVT: 6.43 [SD, 1.71] minutes versus MA-EVT: 3.98 [SD, 1.84] minutes; $P < .001$) (Fig 3).

Robot-Experienced versus Robot-Novice Interventionalists

To assess the impact of the operator's prior experience in the use of the robot, we compared outcomes in experiments performed by robot-experienced ($n = 24$) and robot-novice ($n = 13$) interventionalists (Online Supplemental Data). The observed recanalization rates were 95.8% among the robot-experienced interventionalist and 76.9% among the robot-novice interventionalist ($P = .225$). No significant differences were observed in terms of total emboli count ($P = .065$) or number of emboli of >1 mm ($P = .488$). However, the mean procedural length was found to be slightly-but-significantly longer for robot-experienced (6.85 [SD, 1.54] minutes) compared with robot-novice neurointerventionalists (5.65 [SD, 1.80] minutes; $P = .041$) (Fig 4).

DISCUSSION

In this pilot study, we aimed to characterize the procedural setup and feasibility of performing MT with a robotic-assisted device using a 3D vascular model. We determined that the current robotic features allow an adequate setup to perform RA-EVT in intracranial occlusions located up to the proximal segments on the M2 MCA branches using BGCs and an SR. Thus, patient anatomy should allow navigation of the BGC up to the C2–C3 segments of the ICA. In these conditions, intracranial RA-EVTs performed by physicians with different levels of expertise in the use of the robot were able to achieve similar recanalization rates compared with MA-EVT. RA-EVT may not appear to provide a substantial advantage on its own; however, the current results present opportunities for future scenarios in which skilled neurointerventionalists could potentially perform the intracranial part

of a MT remotely on patients located in distant centers without specialized interventionalists.

In our study, the mean procedural time was slightly higher in the robotic arm compared with the manual procedure, particularly among physicians with experience in robotic procedures. However, in a potential scenario of remote RA-EVT, the absolute increase in the RA procedural time could be neglected if compared with the delays associated with transferring a patient to a comprehensive stroke center to receive EVT.

Furthermore, we aimed to test the safety of the procedure in terms of generation of distal emboli. Overall, our study showed that the total count of generated distal emboli is similar between RA-EVT and MA-EVT. However, we observed a significantly higher number of emboli of >1 mm in the RA-EVT group, which deserves special attention. These results may have been influenced by the use of a 3D plastic model because the friction coefficients between the clot/devices and the vessels are higher than those in human arteries. However, we cannot exclude the possibility that this high rate of clots of >1 cm may be due to the operator's lack of experience with the robot, including performing a procedure in the absence of haptic feedback. Nevertheless, we believe that in the preliminary phases of developing a device, it is important to collect data on the physician's performance with the device, because the data may provide insight into characteristics of the device and help identify areas for improvement. We anticipate that both operator experience and device performance can be improved in the future.

A possible explanation may lie in the relative absence of compliance with the current version of the robotic system when pushing the microcatheters across the thrombus. During manual procedures, the interventionalist can modulate the applied force to gradually advance the microcatheter, avoiding sudden tension releases of the system; however, this step may be more challenging with RA-EVT. Sudden tension releases of the system may also be exacerbated by the increased vessel wall friction of the 3D models compared to a patient's arteries. However, robotic systems have the potential to include automatic compensation and adjustment systems with the ability to optimize microcatheter navigation through the occluding clots.

Most interesting, expert physicians in robot handling achieved results similar to those of physicians with limited robotic exposure (Fig 4), suggesting that spreading this new technology with short learning curves among neurointerventionalists may be relatively straightforward.

Future developments of regional networks will likely consider performing a local MT by an interventionalist not dedicated to neuroendovascular procedures or opting for a remote RA-EVT performed by skilled neurointerventionalists to ensure universal and timely endovascular treatment of patients with stroke with large-vessel occlusions.

To our knowledge, this is the first study that explores the feasibility of robotic assistance in the intracranial part of the MT. Our results suggest that further adjustments will make implementation of this technology possible in assisting acute ischemic procedures in rural areas, thus massively reducing workflow times.

The current CorPath GRX technology still presents limitations that prevent the immediate application of the studied model in clinical practice: It is currently unable to perform the catheterization of

the supra-aortic trunks and deliver the microcatheter up to the clot occlusion. Moreover, the main limitation is the limited range of motion and the impossibility of controlling triaxial catheter systems, preventing the use of intermediate distal-access catheters that provide support during microcatheter navigation and allow distal aspiration.

Our pilot study aimed to provide a preliminary assessment of the feasibility of technology to assist in performing intracranial MT and to generate initial efficacy data. Our results are promising and represent a necessary step toward the implementation of robotics in MT procedures. In the future, integration of acquired vessel imaging, such as CTA or angiography, with the robotic system may enable the robot to recognize the anatomy and offer an assisted navigation in cases of challenging anatomy. Such development allowing a faster, more precise, and safer procedure may facilitate the expansion of an adoption of robotic procedures among less experienced operators or for remote assistance in rural regions.

Limitations

Our study has several limitations. A limited number of operators participated in the study, which may have affected the comparability of the observed outcomes among the various study groups. However, the operators—each having a varying level of experience—conducted multiple experiments to simulate multiple scenarios. Another important limitation is the use of a single 3D printed model, which is a significant constraint due to its limited comparability with real patients. Despite the neurovascular model being internally coated with hydrophilic agents, the friction coefficients between the clot/devices and the vessels are generally higher than those observed in human arteries. This difference may partially explain the increased number and size of distal emboli observed in the RA-EVT arm. Additionally, the model exhibits higher resistance to perforation than in vivo conditions, which hinders the assessment of such complications. Furthermore, a single 3D model was used precluding the wider evaluation according to anatomic variations. We concur with the importance of further exploring the use of robotics to support the catheterization of challenging anatomies in future studies with new iterations of the robotic devices.

CONCLUSIONS

In a 3D printed neurovascular model, RA-EVT has the potential to achieve recanalization rates comparable with MA-EVT within competitive procedural times. Optimization of the procedural setup is still required before implementation in clinical practice.

Disclosure forms provided by the authors are available with the full text and PDF of this article at www.ajnr.org.

REFERENCES

1. Majoie CB, Cavalcante F, Gralla J, et al; IRIS Collaborators. **Value of intravenous thrombolysis in endovascular treatment for large-vessel anterior circulation stroke: individual participant data meta-analysis of six randomised trials.** *Lancet* 2023;402:965–74 [CrossRef Medline](#)
2. Kamel H, Parikh NS, Chatterjee A, et al. **Access to mechanical thrombectomy for ischemic stroke in the United States.** *Stroke* 2021; 52:2554–61 [CrossRef Medline](#)
3. Perez de la Ossa N, Abilleira S, Dorado L, et al; Catalan Stroke Code and Reperfusion Consortium. **Access to endovascular treatment in**

- remote areas: analysis of the Reperfusion Treatment Registry of Catalonia. *Stroke* 2016;47:1381–84 [CrossRef Medline](#)
4. El Nawar R, Lapergue B, Piotin M, et al; ETIS Investigators. Higher annual operator volume is associated with better reperfusion rates in stroke patients treated by mechanical thrombectomy: the ETIS Registry. *JACC Cardiovasc Interv* 2019;12:385–91 [CrossRef Medline](#)
 5. Mahmud E, Schmid F, Kalmar P, et al. Feasibility and safety of robotic peripheral vascular interventions: results of the RAPID Trial. *JACC Cardiovasc Interv* 2016;9:2058–64 [CrossRef Medline](#)
 6. Mendes Pereira V, Rice H, De Villiers L, et al. Evaluation of effectiveness and safety of the CorPath GRX robotic system in endovascular embolization procedures of cerebral aneurysms. *J Neurointerv Surg* 2023 Oct 4. [Epub ahead of print] [CrossRef Medline](#)
 7. Karas PJ, Lee JE, Frank TS, et al. Robotic-guided direct transtemporal embolization of an indirect carotid cavernous fistula. *J Neurointerv Surg* 2023;15:1122–23 [CrossRef Medline](#)
 8. Kikinis R, Piper S, Vosburgh, K. 3D Slicer: A Platform for Subject-Specific Image Analysis, Visualization, and Clinical Support. In: Jolesz FA. *Introperative Imaging and Imaging-Guided Therapy*. Springerlink; 2014:277–89
 9. Fedorov A, Beichel R, Kalpathy-Cramer J, et al. 3D Slicer as an image computing platform for the Quantitative Imaging Network. *Magn Reson Imaging* 2012 Nov;30(9):1323–41 [CrossRef Medline](#)
 10. Autodesk MeshMixer. <https://meshmixer.com/download.html>.
 11. Kan I, Yuki I, Murayama Y, et al. A novel method of thrombus preparation for use in a swine model for evaluation of thrombectomy devices. *AJNR Am J Neuroradiol* 2010;31:1741–43 [CrossRef Medline](#)
 12. Li J, Tiberi R, Canals P, et al. Double stent-retriever as the first-line approach in mechanical thrombectomy: a randomized in vitro evaluation. *J Neurointerv Surg* 2023;15:1224–28 [CrossRef Medline](#)
 13. Li J, Tiberi R, Bhogal P, et al. Impact of stent-retriever tip design on distal embolization during mechanical thrombectomy: a randomized in vitro evaluation. *J Neurointerv Surg* 2023;16:285–89 [CrossRef Medline](#)